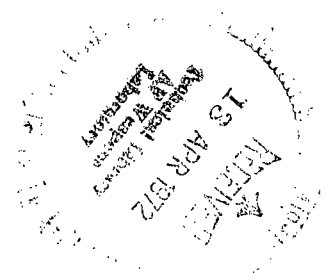# NASA TECHNICAL NOTE

NASA TN D-6581
c.1

NASA TN D-6581

IMPROVED METHODS OF PERFORMING COHERENT OPTICAL CORRELATION

by Akram S. Husain-Abidi

Goddard Space Flight Center
Greenbelt, Md. 20771

NATIONAL AERONAUTICS AND SPACE ADMINISTRATION • WASHINGTON, D. C. • APRIL 1972

0133350

1. Report No. TN D-6581	2. Government Accession No.	3. Recipient's Catalog No.
4. Title and Subtitle Improved Methods of Performing Coherent Optical Correlation		5. Report Date April 1972
		6. Performing Organization Code
7. Author(s) Akram S. Husain-Abidi		8. Performing Organization Report No. G-0000
9. Performing Organization Name and Address Goddard Space Flight Center Greenbelt, Maryland 20771		10. Work Unit No.
		11. Contract or Grant No.
12. Sponsoring Agency Name and Address National Aeronautics and Space Administration Washington, D.C. 20546		13. Type of Report and Period Covered Technical Note
		14. Sponsoring Agency Code
15. Supplementary Notes		

16. Abstract

Coherent optical correlators are described in which complex spatial filters are recorded by a quasi-Fourier transform method. The high-pass spatial filtering effects (due to the dynamic range of photographic films) normally encountered in Vander Lugt type complex filters are not present in this system. Experimental results for both transmittive as well as reflective objects are presented. Experiments are also performed by illuminating the object with diffused light. A correlator using paraboloidal mirror segments as the Fourier-transforming element is also described.

17. Key Words Suggested by Author Optical Correlator Autocorrelation Pattern Recognition System	18. Distribution Statement Unclassified—Unlimited		
19. Security Classif. (of this report) Unclassified	20. Security Classif. (of this page) Unclassified	21. No. of Pages 12	22. Price $3.00

CONTENTS

IMPROVED METHODS OF PERFORMING
COHERENT OPTICAL CORRELATION

by
Akram S. Husain-Abidi*
Goddard Space Flight Center

INTRODUCTION

Vander Lugt's technique (Reference 1) of realising a complex spatial filter was largely responsible for a reevaluation of optical spatial filtering techniques for shape recognition and signal detection in a noisy background. The complex spatial filter, in its simplest form, is a record of the amplitude as well as the phase of the signal information; the information is normally recorded on a single photographic plate that is sensitive only to intensity (the square of the amplitude). The salient feature of this technique is the transformation of phase and amplitude information into intensity information. The two methods reported by Vander Lugt for recording complex valued function on photographic films employ modified Mach-Zehnder and Rayleigh interferometric arrangements. By placing this complex filter in the Fourier transform (or frequency) plane and performing an inverse Fourier transform of the light transmitted by this filter, the autocorrelation (or cross-correlation) function can be obtained. Since in the correlation plane the autocorrelation function of a pattern or shape has a bright central peak, pattern recognition can be achieved by detecting the bright spot.

The purpose of this report is to describe the use of a quasi-Fourier transform hologram technique for recording both amplitude and phase of the signal information and its use in an optical correlator. This system offers greater sensitivity and selectivity than the systems using Fourier transform holograms as complex spatial filters. The high-pass spatial filtering effects due to the dynamic range of photographic films and which are normally encountered in Vander Lugt type complex spatial filters are not present. Effects of diffused illumination in the recordings of complex spatial filter are presented. A correlation system in which paraboloidal mirror segments are used for Fourier-transforming purposes is also described. The advantages of paraboloidal mirror segments over lenses are presented.

SYNTHESIS OF THE COMPLEX SPATIAL FILTER

Figure 1 illustrates the recording arrangements of a complex spatial filter. Since a complex spatial filter of any kind is by definition a hologram, the recording arrangement is similar to that reported

---

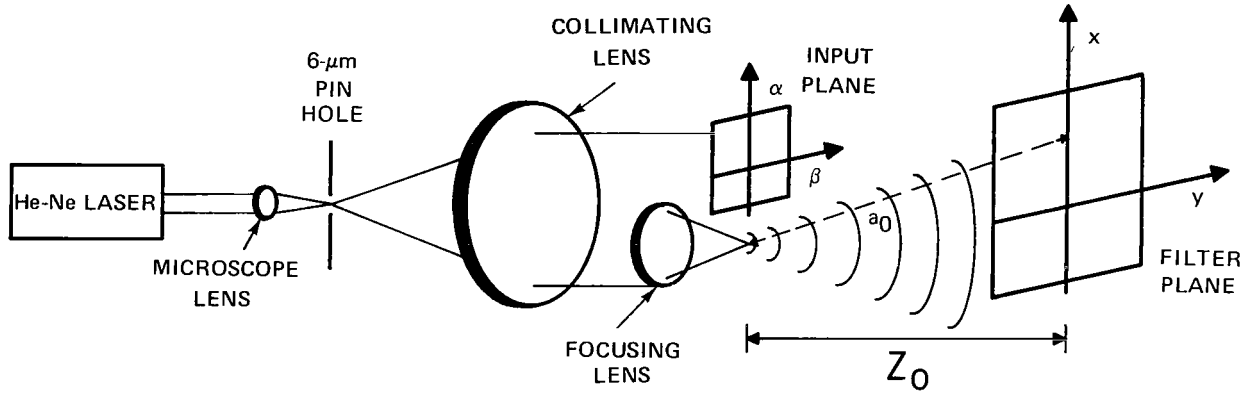*Postdoctoral Resident Research Associate of the National Academy of Sciences.

Figure 1—Recording geometry of a complex spatial filter (or, the lensless Fourier-transform hologram).

by Stroke (Reference 2). The reference beam is a spherical wave diverging from a point source located at the origin in the $\alpha\beta$-plane. If the recording film is placed a distance z_o from the xy-plane, which is parallel to the $\alpha\beta$-plane, the complex amplitude produced by the spherical waves in the xy-plane can be written

$$E_r(x,y) = \frac{A_o e^{jka_o}}{a_o},$$

(1)

where $k = 2\pi/\lambda$.

Under the experimental conditions used to record this complex filter, the term a_o in the denominator of Equation 1 can simply be replaced by z_o. In the exponent however, a_o can not be replaced by z_o, because of the presence of the wave number k, which is large enough that any resulting error multiplied by it would generate phase errors much greater than 2π radians. Again with reference to Figure 1, the exact distance a_o is

$$a_o = \sqrt{z_o^2 + x^2 + y^2}$$

$$= z_o \sqrt{1 + \frac{x^2}{z_o^2} + \frac{y^2}{z_o^2}} .$$

(2)

Since the binomial expansion of the square root is

$$\sqrt{1 + b} = 1 + \tfrac{1}{2}b - \tfrac{1}{8}b^2 + \cdots \quad \text{for} \quad |b| < 1 ,$$

Equation 2 can be written

2

$$a_o \approx z_o \left(1 + \frac{x^2 + y^2}{2z_o^2} \right) . \tag{3}$$

Therefore, Equation 1 can be written

$$E_r(x,y) = \frac{1}{z_o} \exp\left[jkz_o \left(1 + \frac{x^2 + y^2}{2z_o^2} \right) \right] . \tag{4}$$

Consider an object transparency (or any reflecting object) placed in the $\alpha\beta$-plane such that the object and reference point are coplanar. If the object is illuminated by a plane wave of unit amplitude at normal incidence and if the transmittance (or reflectance) of the object is $t(\alpha,\beta)$, then, according to Fresnel diffraction, the field in the xy-plane can be written

$$E_s(x,y) = \frac{e^{jkz_o}}{j\lambda z_o} \iint\limits_{-\infty}^{+\infty} t(\alpha,\beta) \exp\left\{ \frac{jk}{2z_o} [(x-\alpha)^2 + (y-\beta)^2] \right\} d\alpha\, d\beta . \tag{5}$$

From Equations 4 and 5, the total intensity $I(x,y)$ recorded on photographic film in the xy-plane can, therefore, be written

$$I(x,y) = |E_r(x,y) + E_s(x,y)|^2$$

$$= |E_r(x,y)|^2 + |E_s(x,y)|^2 + E_r(x,y)E_s^*(x,y) + E_r^*(x,y)E_s(x,y) , \tag{6}$$

where the asterisk (*) signifies the complex conjugate. By putting the appropriate values for $E_r(x,y)$ and $E_s(x,y)$ in the last two terms of Equation 6, we get

$$I(x,y) = |E_r(x,y)|^2 + |E_s(x,y)|^2 + \frac{1}{j\lambda z_o^2} \iint\limits_{-\infty}^{+\infty} t^*(\alpha,\beta) \exp\left[\frac{jk}{z_o}(x\alpha + y\beta) \right] \exp\left[-\frac{jk}{2z_o}(\alpha^2 + \beta^2) \right] d\alpha\, d\beta$$

$$+ \frac{1}{j\lambda z_o^2} \iint\limits_{-\infty}^{+\infty} t(\alpha,\beta) \exp\left[-\frac{jk}{z_o}(x\alpha + y\beta) \right] \exp\left[\frac{jk}{2z_o}(\alpha^2 + \beta^2) \right] d\alpha\, d\beta . \tag{7}$$

Equation 7 shows the way in which amplitude and phase information can be recorded on intensity-sensitive photographic films as amplitude and phase modulations of a "high-frequency carrier" introduced by the reference beam's emerging from a point source.

The final step in the synthesis of a complex spatial filter is to develop the exposed film to produce a transparency. The transmittance τ of the developed film is proportional to the intensity distribution of the exposing field during exposure; therefore,

$$\tau(x,y) \sim I(x,y) , \tag{8}$$

which is defined by Equation 7. After synthesizing the complex spatial filter, it was placed in the optical system (described in the next section) for data processing.

PROCESSING THE INPUT DATA

The complex spatial filter was returned to the position in which it was recorded. When this filter is illuminated by the field produced by the original transparency, the field strength $\mathcal{E}_2$ transmitted will obey the proportionality

$$\mathcal{E}_2 \sim E_{\bar{s}}[I(x,y)] \ . \tag{9}$$

Lens L_4 of Figure 1 Fourier transforms $\mathcal{E}_2$; therefore, the field strength $\mathcal{E}_3$ in the focal plane of the lens will be

$$\mathcal{E}_3 \alpha\, \mathcal{F}\left\{E_s[|E_r(\alpha,\beta)|^2 + |E_s(\alpha,\beta)|^2]\right\}$$

$$+ \frac{1}{(jkz_o^2)^2} \iiiint\limits_{-\infty}^{+\infty} t^*(\bar{\alpha},\bar{\beta})t(\alpha,\beta) \exp\left[\frac{jk}{z_o}(x\bar{\alpha} + y\bar{\beta})\right] \exp\left[-\frac{jk}{2z_o}(\bar{\alpha}^2 + \bar{\beta}^2)\right]$$

$$\cdot \exp\left\{\frac{jk}{2z_o}[(x-\alpha)^2 + (y-\beta)^2]\right\} \exp\left[-\frac{jk}{f}(xx_1 + yy_1)\right] d\alpha\, d\beta\, d\bar{\alpha}\, d\bar{\beta}\, dx_1\, dy_1$$

$$+ \frac{1}{(jkz_o^2)^2} \iiiint\limits_{-\infty}^{+\infty} t(\alpha,\beta)t(\bar{\alpha},\bar{\beta}) \exp\left[-\frac{jk}{z_o}(x\bar{\alpha} + y\bar{\beta})\right] \exp\left[\frac{jk}{2z_o}(\bar{\alpha}^2 + \bar{\beta}^2)\right]$$

$$\cdot \exp\left\{\frac{jk}{2z_o}[(x-\alpha)^2 + (y-\beta)^2]\right\} \exp\left[-\frac{jk}{f}(xx_1 + yy_1)\right] d\alpha\, d\beta\, d\alpha'\, d\beta'\, dx_1\, dy_1\ , \tag{10}$$

where $\mathcal{F}$ represents the Fourier transform and f is the focal length.

The first term in Equation 10 contains the geometrical image of $t(\alpha,\beta)$. Let us consider the second term, which can be written

$$\frac{1}{(jkz_o^2)^2} \iiiint\int\int t^*(\bar{\alpha},\bar{\beta})t(\alpha,\beta) \exp\left[-\frac{jk}{2z_o}(\bar{\alpha}^2 + \bar{\beta}^2)\right] \exp\left[\frac{jk}{2z_o}\left(2x\bar{\alpha} + 2y\bar{\beta}\right.\right.$$

$$\left.\left. + x^2 + \alpha^2 - 2x\alpha + y^2 + \beta^2 - 2y\beta - \frac{2z_o}{f}xx_1 - \frac{2z_o}{f}yy_1\right)\right] d\alpha\, d\beta\, d\bar{\alpha}\, d\bar{\beta}\, dx\, dy\ , \tag{11}$$

or

$$\frac{1}{(jkz_o^2)^2} \iiiint t^*(\bar{\alpha},\bar{\beta})t(\alpha,\beta) \exp\left[-\frac{jk}{2z_o}(\bar{\alpha}^2+\bar{\beta}^2)\right] \exp\left[\frac{jk}{2z_o}(\alpha^2+\beta^2)\right] \exp\left[\frac{jk}{2z_o}(x^2+y^2)\right]$$

$$\cdot \exp\left\{-\frac{jk}{z_o}\left[x\left(\alpha-\bar{\alpha}+\frac{z_o}{f}x_1\right)+y\left(\beta-\bar{\beta}+\frac{z_o}{f}y_1\right)\right]\right\} d\alpha\, d\beta\, d\bar{\alpha}\, d\bar{\beta}\, dx\, dy \ . \tag{12}$$

The most troublesome terms in Equation 12 are those containing the quadratic phase factor. These terms are only indicative of phase curvature over the $\alpha\beta$- and xy-planes and, for most cases of interest, can be dropped. Therefore, Equation 12 can be written as

$$\frac{1}{(jkz_o^2)^2} \iiiint t^*(\bar{\alpha},\bar{\beta})t(\alpha,\beta)$$

$$\cdot \exp\left\{-\frac{jk}{z_o}\left[x\left(\alpha-\bar{\alpha}+\frac{z_o}{f}x_1\right)+y\left(\beta-\bar{\beta}+\frac{z_o}{f}y_1\right)\right]\right\} d\alpha\, d\beta\, d\bar{\alpha}\, d\bar{\beta}\, dx\, dy \ . \tag{13}$$

After integrating over x, y, $\bar{\alpha}$, and $\bar{\beta}$, we obtain

$$\frac{1}{jkz_o^2} \iint t(\alpha,\beta)t^*\left(\alpha+\frac{z_o}{f}x_1, \beta+\frac{z_o}{f}y_1\right) d\alpha\, d\beta \ . \tag{14}$$

Equation 14 can be recognized as the autocorrelation function of $t(\alpha,\beta)$.

Similarly, the third term of Equation 10, when reduced, can be recognized as the convolution of $t(\alpha,\beta)$.

OPTICAL CORRELATORS

Figures 2, 3, and 4 illustrate the experimental arrangements used to perform autocorrelation. In all three systems, coherent illumination was provided by an He-Ne gas laser radiating at 6238Å wavelength. The light from the laser was brought to a point focus by a microscope objective. A 6-μm-diameter aperture was placed in the focal plane to eliminate laser beam noise and to exclude stray light. In two of the arrangements (Figures 2 and 3), another lens was placed a focal length away from the focal plane to collimate the laser light. In the third arrangement (Figure 4), an off-axis paraboloidal mirror segment was used to collimate the laser beam.

Let us consider Figure 2 in detail. A portion of the collimated light was brought to focus in the $\alpha\beta$-plane to act as a point reference source for recording the complex spatial filter. The rest of the collimated light was allowed to impinge upon a transparency, which was also located in the $\alpha\beta$-plane.
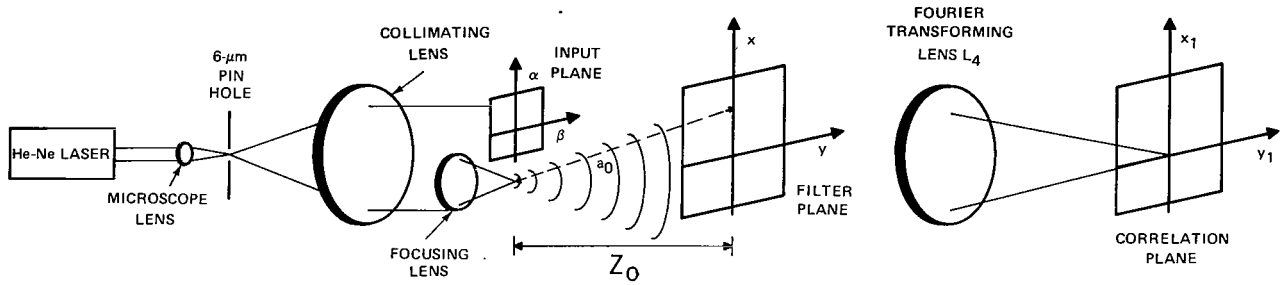
5

Figure 2—Optical correlator for transmittive objects.

The interference fringes produced by the field scattered by the object transparency and the spherical waves originating from the point source (which was coplaner with the object transparency) were recorded on a photographic film in the xy-plane, which was located a distance z_o from the $\alpha\beta$-plane. Another lens (L_4) was placed a focal length away from the xy-plane, and this lens was used to Fourier transform the field distribution transmitted by the developed complex spatial filter. The correlation spot was monitored in the x_1y_1-plane.

The experimental arrangement shown in Figure 3 was used for correlography of reflective objects. The collimated light was split into two parts by an optical wedge, used to avoid the front surface reflections. The first part of the collimated beam was directed toward the object (which was placed in the $\alpha\beta$-plane) by front-surface reflecting mirrors (M_1, M_2, M_3, and M_4). Mirrors M_5, M_6, and M_7 and lens L_3 were used to direct and focus the second part of the beam in the form of a point source in the $\alpha\beta$-plane. This focused light in the $\alpha\beta$-plane was used as a point source of spherical waves for recording the complex spatial filter. The phase and amplitude information of the object was recorded in terms of interference fringes in the xy-plane. The photographic plate was developed and placed in exactly the same position it occupied during the exposure. Lens L_4 Fourier transformed the field transmitted by the complex spatial filter when illuminated by the diffraction field produced by the object in the $\alpha\beta$-plane. The autocorrelation spot was monitored in the x_1y_1-plane.

In the experimental arrangement of Figure 4, the laser light was brought to focus by a microscope objective and then spatially filtered by a 6-μm-diameter pin hole. An off-axis paraboloidal mirror segment (M_1) was used to collimate the laser light. A portion of the collimated light was diverted by a front-surface reflecting mirror (M_1) toward an off-axis paraboloidal mirror segment (M_2) that focused the beam in the $\alpha\beta$-plane. The spherical waves produced by this point source were used as the reference beam. The remaining portion of the collimated light was brought to the $\alpha\beta$-plane by means of mirrors M_2 and M_3. The input transparency was placed in this plane, and the complex spatial filter was recorded in the xy-plane.

Another off-axis paraboloidal mirror segment Fourier transformed the field transmitted by the developed complex spatial filter when illuminated by the field produced by the input transparency. The correlation function was monitored in the x_1y_1-plane.
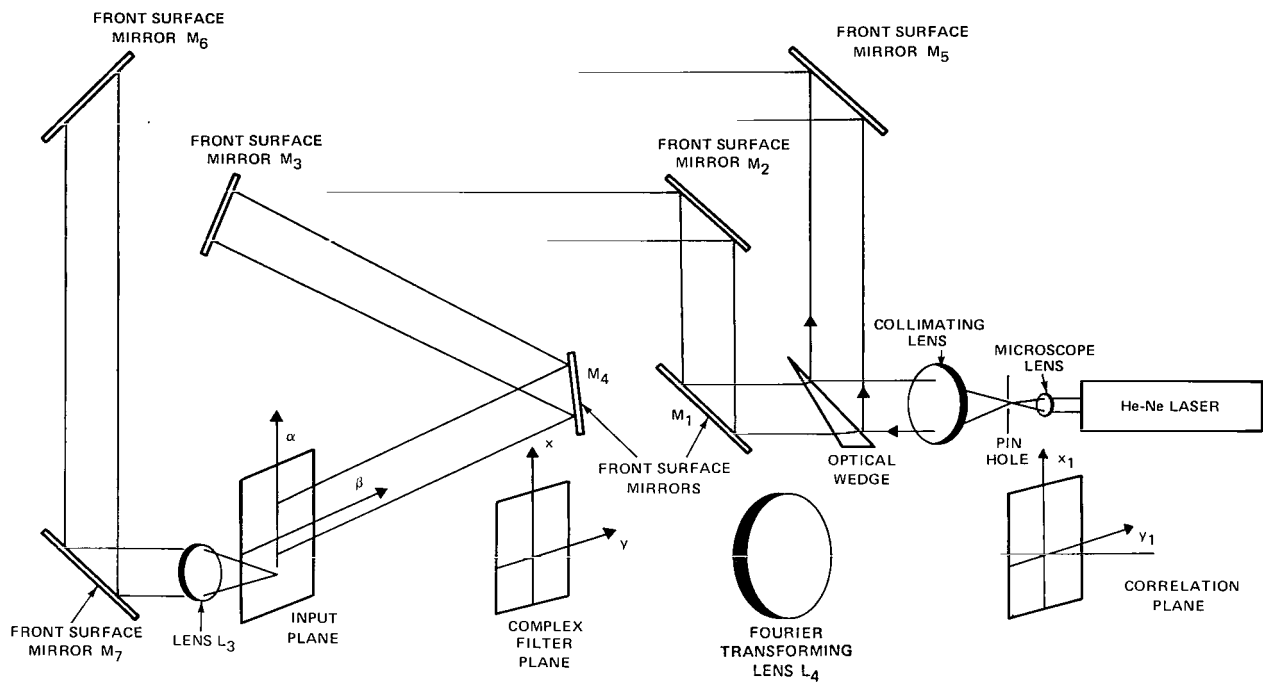
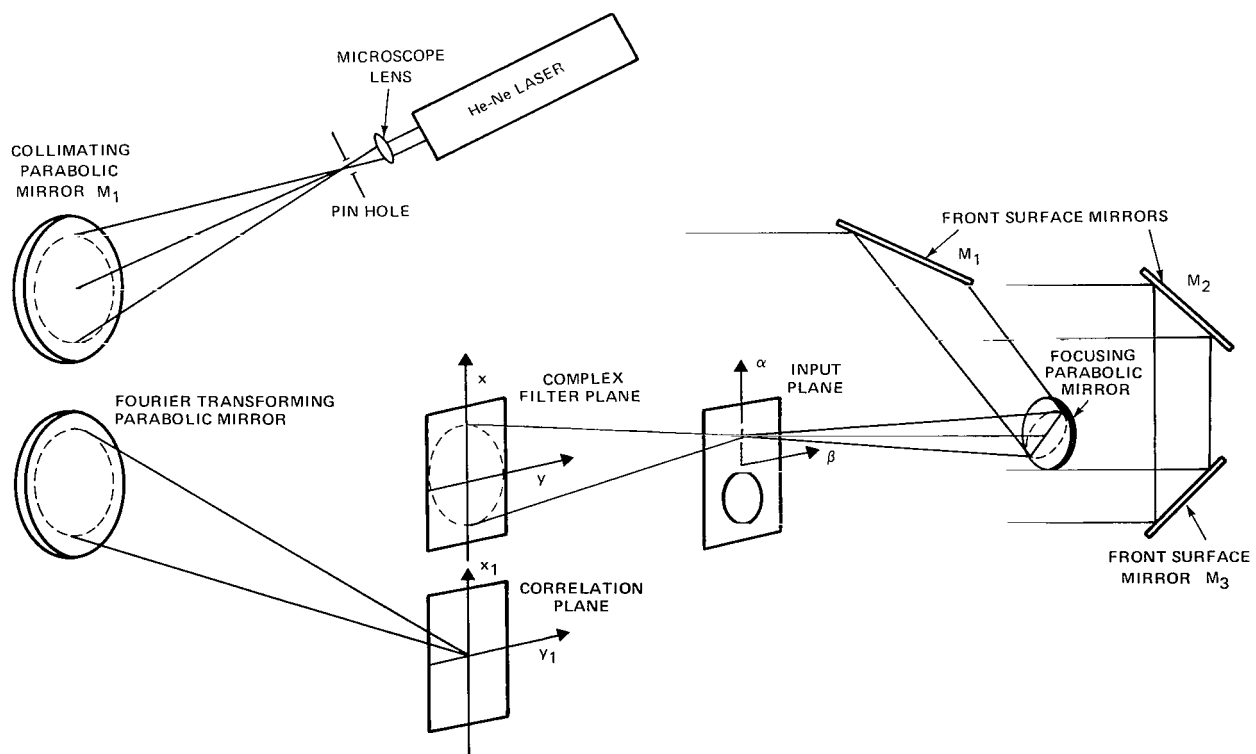Figure 3—Optical correlator for reflective objects.

Figure 4—Optical correlator for transmittive objects using paraboloidal mirror segments.

The use of parabolic mirrors in this arrangement has a number of advantages over a correlator with lenses. The absence of paraxial approximation in the derivation of the transfer function for a parabolic mirror indicates that the focal length of the parabolic mirror is not a function of the index of refraction; hence, all rays parallel to the optical axis of a parabolic mirror intersect at the focal point. This independence from the refractive index means that material for fabrication of the mirrors need not to be homogeneous and isotropic. Therefore, the use of paraboloidal mirror overcomes all the critical limitations on optical material. Also, the aperture for the optical signal being processed can be larger for a parabolic mirror than for a lens of the same diameter. More importantly, off-axis segments of the parabolic mirror can be used as optical-system elements since these segments have the same transforming properties of the original mirror and the same relative axis. Thus, a folded optical system can be designed. The use of parabolic mirrors has an added advantage in that they do not generate front-surface reflections.

EXPERIMENTAL RESULTS

Transmittive Objects

Operation of the experimental arrangement to perform autocorrelation on transmittive objects has been described in the preceding sections. For the experiment, photographic transparency of a brain tissue was chosen as an object. The transparency was placed in the $\alpha\beta$-plane, and special care was taken to ensure that the reference point source and the input transparency were coplanar. The photographic plate was placed in the xy-plane. The ratio of the intensity of the reference beam to the light transmitted by the input transparency was typically 1:1. Exposure was controlled such that the transmission of the developed film was in the linear region of the Hurter-Driffield curve. After exposure, the film was developed and returned to the same position it occupied during the exposure. The complex spatial filter (or the hologram) was then illuminated with the light transmitted by the object transparency, and lens L_4 takes the Fourier transform of the field transmitted by the filter. The correlation function, the geometrical image of the input transparency, and the convolution function were recorded in the $x_1 y_1$-plane, as is shown in Figure 5. The autocorrelation function has a characteristic bright central peak and therefore can easily be detected; this bright peak can easily be seen in the photograph.
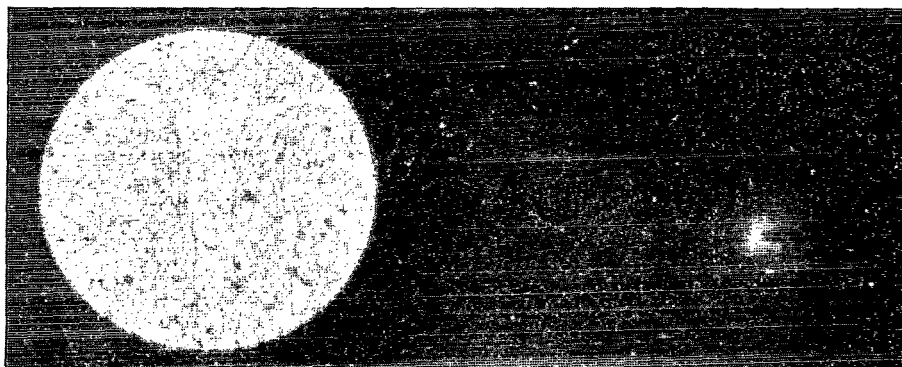

Figure 5—Autocorrelation of brain tissue.

Reflective Objects

Experimental arrangements for reflective objects are far more complicated than those for transmittive objects. (Figure 3 is an example of such system.) The acronym "NASA" was scratched on a black-painted aluminum surface and was used as an object for autocorrelation. The plate was placed in the $\alpha\beta$-plane, and special care was taken to ensure that the light focused by lens L_3 and the front surface of the aluminum plate were coplaner. The photographic plate was placed in the xy-plane. The ratio of the reference beam to light scattered by the object was typically $1:1$. After an experimental procedure similar to that in the previous section was followed, the correlation spot was obtained in the $x_1 y_1$-plane; Figure 6 is a photograph of that plane. The geometrical image of NASA and the bright central peak of the autocorrelation function can be seen in the photograph; Figure 7 shows the impulse response of the complex spatial filter.

The effect of the displacement of the input information in the $\alpha\beta$-plane on the correlation spot in the $x_1 y_1$-plane was investigated by placing a vidicon tube in the $x_1 y_1$-plane. The output of the vidicon tube was simultaneously displayed on a television monitor and on an oscilloscope. When the input information was displaced in either the α- or the β-direction, the correlation spot was found to lose its brightness and move with respect to the movement of the object in the $\alpha\beta$-plane.

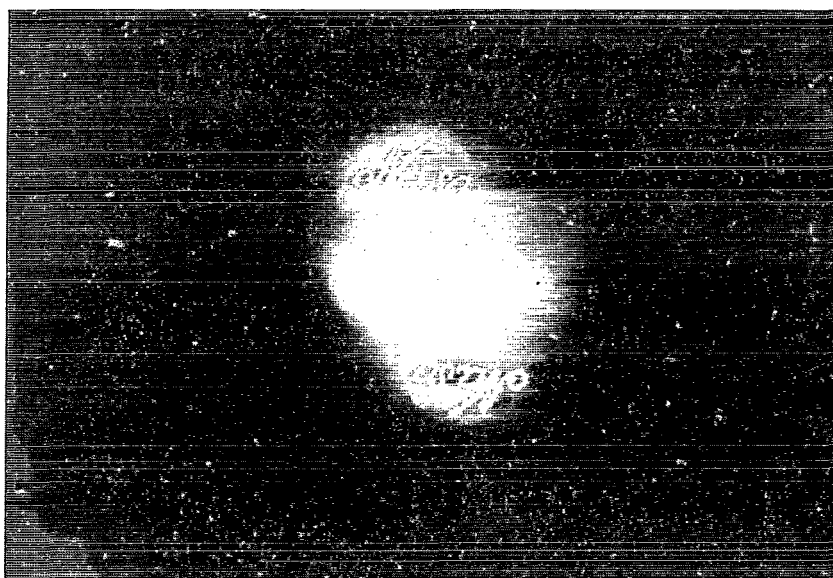Figure 6—Autocorrelation of a reflective object. Photograph of the $x_1 y_1$-plane.

9

Figure 7—Impulse response of the complex spatial filter of the acronym "NASA".

Figure 8a is an oscilloscope trace of the composite video signal of the cross-correlation (30 lines in the center of the frame are shown). Figures 8b and 8c show the scanned cross-correlation spot when the transparent object was displaced 2 and 3 mm respectively in the $+\beta$-direction. Figure 8d shows the scanned cross-correlation spot when the object was displaced 3 mm in the $-\beta$-direction.

EFFECTS OF DIFFUSE ILLUMINATION

The concept of diffuse illumination holography, first introduced by Leith and Upatnicks (Reference 3), has some very interesting advantages. The laser light was diffused by placing an opal glass just behind the object transparency in the experimental arrangement of Figure 2. The light thus diffused behaves in some ways as if it were incoherent, but it retains the time-invarient property of the amplitude and phase relationship. This property is responsible for the recording of the hologram and is absent in the case of incoherent illumination.

One of the many advantages of recording holograms by diffusing the light that illuminates the object is that the diffuse illumination causes each point of the object to radiate a spherical wave; therefore, the information regarding each point of the object is spread over the entire photographic plate. This eliminates any recognizable shadows of the object on the photographic plate. Also, the effects of microscopic imperfection in or on the surface of such optical components as mirrors, beamsplitters, and lenses are minimized because the results of imperfections are smeared over the entire recording plate, resulting in negligibly small mean effects. The effects of dirt or scratches can similarly be made insignificantly small. The minimization of all these effects results in better sensitivity and selectivity for the optical correlators.
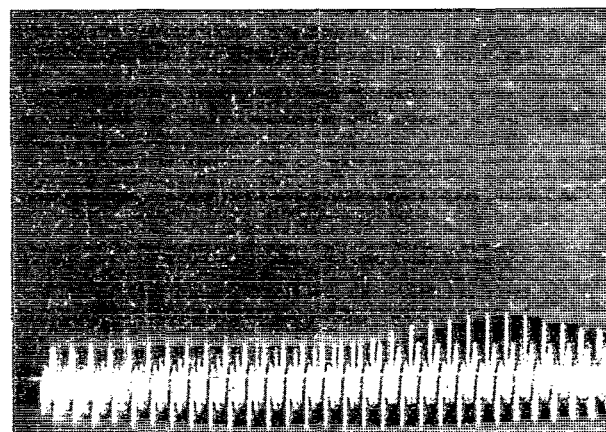
10
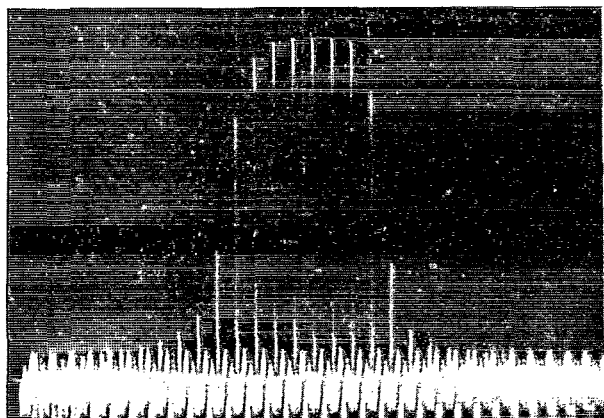
(a) Zero displacement.
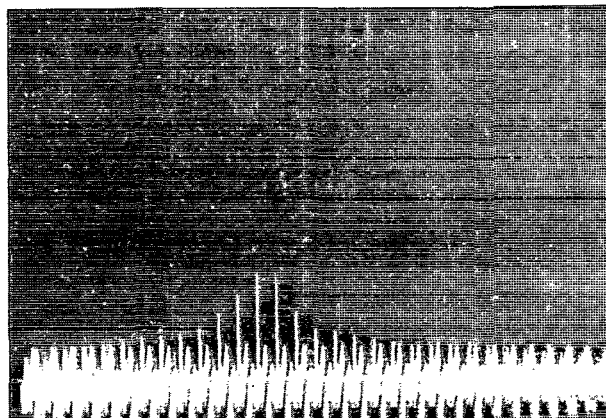
(b) 2-mm displacement in the $+\beta$ direction.
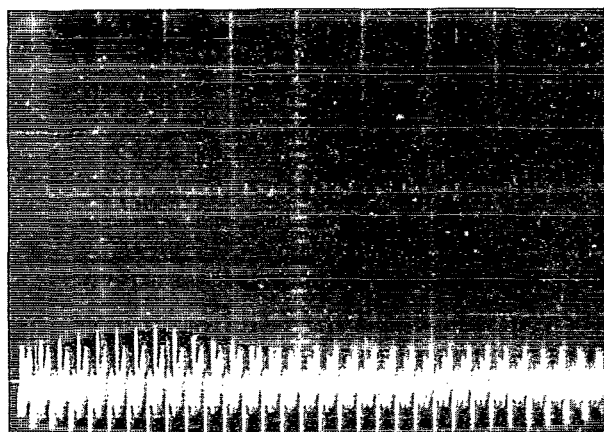
(c) 3-mm displacement in the $+\beta$ direction.

(d) 3-mm displacement in the $-\beta$ direction.

Figure 8—Composite video signal of the cross-correlation for the measure of the displacement of the input information.

CONCLUSIONS

The coherent optical correlator using a quasi-Fourier transform method of recording complex spatial filters is a highly sensitive and selective system since these correlators display the true correlation value at only a single point (i.e., where the correlation spot has the maximum value). The other advantage is in the flexibility in the recording of the complex spatial filter. In a quasi-Fourier transform method of recording phase and amplitude information there is a one-to-one correspondence between the object coordinates and the spatial frequencies at the hologram (to be used as a complex spatial filter), and the information can be recorded on low-resolution recording materials. Also, the high-pass spatial filtering effects normally encountered in Vander Lugt type complex spatial filters due to the limited dynamic range of photographic films are not present in these systems.

It has also been shown that by placing a diffuser just behind the object transparency, the quality of the complex spatial filter can be improved.

ACKNOWLEDGMENT

The author wishes to express his appreciation to Mr. David H. Schaefer for his interest and encouragement.

REFERENCES

1. Vander Lugt, A. B., "Signal Detection by Complex Spatial Filtering," IEEE Trans. Information Theory, IT-10:2, 139 (1964).

2. Stroke, G. W., "Lensless Fourier-Transform Method for Optical Holography," *Appl. Phys. Lett.* 6, 201 (1965).

3. Leith, E. N., and Upatnicks, J., "Wavefront Reconstruction With Diffused Illumination and Three-Dimensional Objects," *J. Opt. Soc. Am.* 54, 1295 (1964).

"The aeronautical and space activities of the United States shall be conducted so as to contribute . . . to the expansion of human knowledge of phenomena in the atmosphere and space. The Administration shall provide for the widest practicable and appropriate dissemination of information concerning its activities and the results thereof."

— NATIONAL AERONAUTICS AND SPACE ACT OF 1958

NASA SCIENTIFIC AND TECHNICAL PUBLICATIONS

TECHNICAL REPORTS: Scientific and technical information considered important, complete, and a lasting contribution to existing knowledge.

TECHNICAL NOTES: Information less broad in scope but nevertheless of importance as a contribution to existing knowledge.

TECHNICAL MEMORANDUMS: Information receiving limited distribution because of preliminary data, security classification, or other reasons.

CONTRACTOR REPORTS: Scientific and technical information generated under a NASA contract or grant and considered an important contribution to existing knowledge.

TECHNICAL TRANSLATIONS: Information published in a foreign language considered to merit NASA distribution in English.

SPECIAL PUBLICATIONS: Information derived from or of value to NASA activities. Publications include conference proceedings, monographs, data compilations, handbooks, sourcebooks, and special bibliographies.

TECHNOLOGY UTILIZATION PUBLICATIONS: Information on technology used by NASA that may be of particular interest in commercial and other non-aerospace applications. Publications include Tech Briefs, Technology Utilization Reports and Technology Surveys.

Details on the availability of these publications may be obtained from:

SCIENTIFIC AND TECHNICAL INFORMATION OFFICE

NATIONAL AERONAUTICS AND SPACE ADMINISTRATION
Washington, D.C. 20546